PERGAMON

International Journal of Solids and Structures 36 (1999) 441–464

INTERNATIONAL JOURNAL OF SOLIDS and STRUCTURES

Influence of localized imperfections on the buckling of cylindrical shells under axial compression

M. Jamal[a], M. Midani,[a] N. Damil[a,]*, M. Potier-Ferry[b]

[a]*Laboratoire de Calcul Scientifique en Mécanique, Faculté des Sciences Ben M'sik, Université Hassan II, BP 7955 Sidi Othman, Casablanca, Morocco*

[b]*Laboratoire de Physique et Mécanique des Matériaux, U.R.A.-C.N.R.S. no. 1215, I.S.G.M.P. Université de Metz, Ile du Saulcy, 57045 Metz Cedex 01, France*

Received 24 July 1997

Abstract

The influence of localized imperfections on the buckling of a long cylindrical shell under axial compression is analysed by using a double scale analysis including interaction modes. This leads to a system of coupled complex non-linear differential equations with discontinuous derivatives. We propose analytical formulas to predict the reduction of the critical buckling load.

1. Introduction

The elastic buckling of cylindrical shells under axial compression gave rise to several studies on account of the high imperfection sensitivity of these structures. One of the reasons of this strong sensitivity to shape defects is the existence of a great number of coincident or nearly coincident modes for large value of Batdorf parameter i.e. for sufficiently long and sufficiently thin shells. It is not possible to represent correctly this phenomenon by taking into account only one mode in a postbuckling analysis. Hence Koiter (1963) shows that one must couple three modes to study the influence of axisymmetric imperfections. Several studies, for example Arbocz (1987) have also introduced many modes to analyse the influence of different imperfection shapes correctly.

The postbuckling of these structures have as well been studied by numerical means, usually with simplified codes. Generally, these codes associate a Fourier analysis in the circumferential direction with a spatial discretization in the axial direction (Yamaki (1984), Bushnell (1985), Combescure (1995)). Nevertheless, this direct approach selects some solutions from a great number, which leads to deflections that are periodical in the circumferential direction and not periodical but distributed

* Author to whom correspondence should be addressed.

0020–7683/99/$ - see front matter
PII: S0020–7683(98)00026–2

in the axial direction. Recently, Hunt and Lucena Neto (1991) have proposed a semi-analytical method to obtain localized solutions in the axial direction, by coupling a double scale asymptotic analysis in the axial sense and an approximation using three modes in the circumferential sense.

In this paper, we propose to use the method of the last authors to study the influence, on the buckling load, of localized defects in the axial direction.

It is known, from, Amazigo *et al.* (1970) paper's, that localized defects have not the same influence as the distributed defects and that this problem must be studied by assuming a nearly periodic deflection with slowly varying amplitudes. Applications of this idea have been done for pressurized cylindrical shells, Amazigo and Fraser (1971), Abdelmoula *et al.* (1992), but in this case, it is sufficient to modulate only one mode. Let us note that a general theory has been proposed (Damil and Potier-Ferry (1992)) to take into account the influence of localized and distributed defects in the case of only one instability mode, but, in this study, three modes are needed.

Using a double scale analysis including three modes interaction in the presence of localized imperfections, we get the same three complex coupled non-linear second order differential equations, as in Hunt and Lucena Neto (1991), with discontinuous derivatives in the region where the localized imperfections are significant. The expression of these discontinuities is given in terms of the shape of localized imperfections. We solve numerically these three coupled differential equations by means of the Newton–Raphson method. Based on a scaling analysis, we show that the reduction of the critical load is proportional to $(a_l)^{2/3}$, where a_l is the amplitude of the localized imperfection. We also give an estimation of the coefficient of proportionality.

2. Physical problem and linear analysis

We consider a circular cylindrical shell of radius R, length L and thickness h, which is made of an homogeneous, isotropic, elastic material with Young's modulus E and Poisson's ratio v. It is subjected to an axial compressive load P. The coordinate system is taken as shown in Fig. 1(a)

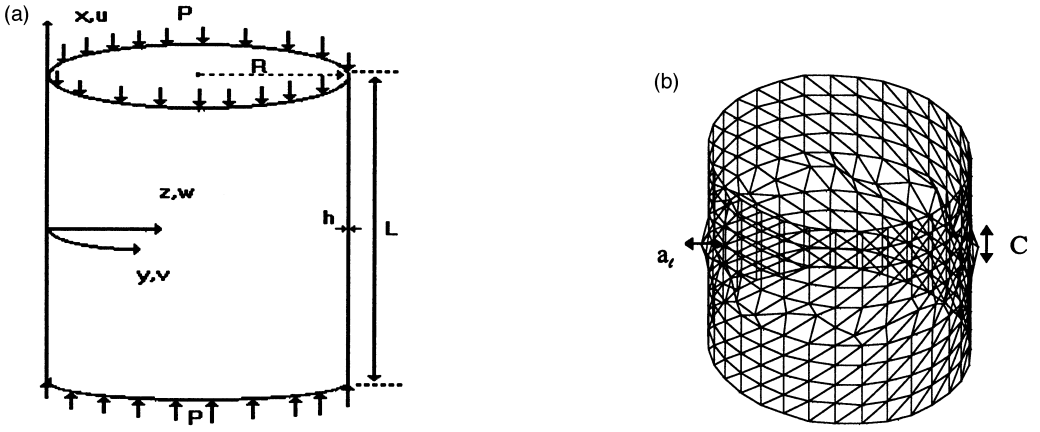

Fig. 1. (a) Cylinder shell subject to a uniform axial compression. (b) Cylindrical shell in presence of a localized imperfection.

and the displacement components will be denoted by u, v and w. Within Donnell theory and if the pre-buckling rotations are neglected, the transverse displacement $w(x, y)$ and the additional stress function $\Phi(x, y)$ are solutions of (Yamaki (1984), Hunt and Lucena Neto (1991))

$$k^2\Delta^2 w+\lambda\left(\frac{\partial^2 w}{\partial x^2}+\frac{\partial^2 d}{\partial x^2}\right)-\rho\frac{\partial^2\Phi}{\partial x^2}=[w+d,\Phi] \tag{1}$$

$$\Delta^2\Phi+\rho\frac{\partial^2 w}{\partial x^2}=\frac{1}{2}[w+d,w+d] \tag{2}$$

where $\lambda = P/Eh$ is the load parameter, $k^2 = h^2/12(1-\nu^2)$, $\rho = 1/R$ is the shell curvature and $d(x, y)$ is the initial imperfection. The stress function Φ is related to the resultant stress by

$$N_x = Eh\frac{\partial^2\Phi}{\partial y^2},\quad N_y = Eh\frac{\partial^2\Phi}{\partial x^2},\quad N_{xy} = -Eh\frac{\partial^2\Phi}{\partial x\,\partial y} \tag{3}$$

Δ^2 denotes the biharmonic operator, and [,] is the usual bracket operator

$$[g,f] = \frac{\partial^2 g}{\partial x^2}\frac{\partial^2 f}{\partial y^2}+\frac{\partial^2 g}{\partial y^2}\frac{\partial^2 f}{\partial x^2}-2\frac{\partial^2 g}{\partial x\,\partial y}\frac{\partial^2 f}{\partial x\,\partial y} \tag{4}$$

We characterize the initial imperfection by its amplitude a_l and by its shape $g_l(x, y)$ as follows

$$\mathrm{d}(x, y) = a_l g_l(x, y),\quad \max|g_l(x, y)| = 1 \tag{5}$$

In addition, we suppose that $g_l(x, y)$ is rapidly decaying for large $|x|$, which means that the imperfection is axially localized near the central circle (Fig. 1(b)).

Within the standard linear theory and without defect, the critical value of the load λ is characterized by the existence of a buckling mode (w, Φ), which is the solution of the linearized equations.

$$k^2\Delta^2 w+\lambda\frac{\partial^2 w}{\partial x^2}-\rho\frac{\partial^2\Phi}{\partial x^2}=0 \tag{6}$$

$$\Delta^2\Phi+\rho\frac{\partial^2 w}{\partial x^2}=0 \tag{7}$$

As we assume that the Batdorf parameter, $Z = L^2\sqrt{1-\nu^2}/Rh$, is sufficiently large, the modes are very oscillating in both axial and circumferential directions (Brush and Almroth (1975), Timoshenko and Gere (1961), Yamaki (1984)). So, in a first approximation, the boundary conditions at the ends of the shell can be replaced by the requirement of a harmonic behaviour in the x-direction. Hence, the packet of buckling modes is expressed as

$$w = A\exp(i\gamma x)\cos\beta\gamma y+\text{c.c.} \tag{8}$$

$$\Phi = A_1\exp(i\gamma x)\cos\beta\gamma y+\text{c.c.} \tag{9}$$

$$\lambda = k^2\gamma^2(1+\beta^2)^2+\frac{\rho^2}{\gamma^2(1+\beta^2)^2} \tag{10}$$

where A is an arbitrary constant, $A_1 = \rho A/\gamma^2(1+\beta^2)^2$ and $\gamma = \rho n/\beta$. The nondimensional number β is the modal aspect ratio (axial/circumferential wavelength), n is the number of waves in the circumferential direction, and c.c. denotes the complex conjugate.

The analytical minimization of λ gives

$$\lambda_c = 2\rho k \tag{11}$$

$$\gamma^2(1+\beta^2)^2 = \frac{\rho}{k} \tag{12}$$

λ_c is the classical Donnel buckling load. Within this classical analysis, there are many coincident modes and the corresponding wavenumbers γ and $\beta\gamma$ are located on the Koiter circle (Fig. 2). Equation (12) is the required condition for the mode (8) to be on the Koiter circle.

Let us remark that the boundary conditions could be reintroduced within the cellular bifurcation theory that will be used in what follows (Newell and Whitehead (1969), Segel (1969), Lange and Newell (1971), Potier-Ferry (1983), Damil and Potier-Ferry (1986)). Nevertheless, it is not necessary to account for boundary conditions in the present study of localized postbuckling.

3. Three coupled amplitude equations

In this section, we solve the non-linear differential problem (1), (2) by using a double scale perturbation analysis. The expansion parameter η is connected with the amplitude of the localized imperfection a_l by:

$$\eta = (a_l)^{2/3} \tag{13}$$

The double scale expansion method is a classical tool to analyse cellular bifurcations, since papers by Segel (1969) and Newell and Whitehead (1969). We introduce the following slowly varying coordinate

$$X = \eta^{1/2} x \tag{14}$$

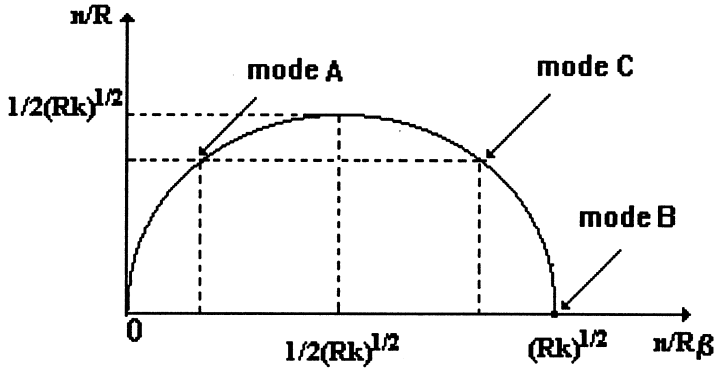

Fig. 2. The Koiter circle: the number of waves in the circumferential direction vs the number of waves in the axial direction.

Thus, x is qualified as a rapidly varying coordinate. In order to simplify, we introduce the following notation

$$\mathbf{u} = \begin{pmatrix} w \\ \Phi \end{pmatrix} \tag{15}$$

We shall assume that the unknown $\mathbf{u}$ is a function of the three "independent" variables X, x, y. According to the classical rule within the double scale expansion method, the following identities hold (for $m = 1, 2, \ldots$)

$$\frac{\partial^m}{\partial x^m} \to \sum_{p=0}^{m} C_m^p \eta^{(m-p)/2} \left(\frac{\partial^p}{\partial x^p}\right)\left(\frac{\partial^{m-p}}{\partial X^{m-p}}\right); \quad C_m^p = \frac{m!}{p!(m-p)!} \tag{16}$$

where $\partial^0/\partial X^0 = \partial^0/\partial x^0 = 1$. The bilaplacien operator Δ^2 will be then replaced by:

$$\Delta^2 + 4\eta^{1/2}\left(\frac{\partial^4}{\partial x^3\,\partial X} + \frac{\partial^4}{\partial x\,\partial X\,\partial y^2}\right) + 2\eta\left(\frac{\partial^4}{\partial X^2\,\partial y^2} + 3\frac{\partial^4}{\partial x^2\,\partial X^2}\right) + 4\eta^{3/2}\frac{\partial^4}{\partial x\,\partial X^3} + \eta^2\frac{\partial^4}{\partial X^4} \tag{17}$$

The unknown $\mathbf{u}$ and the load parameter λ are expanded into powers of η

$$\mathbf{u}(x, X, y) = \eta\mathbf{u}_1(x, X, y) + \eta^{3/2}\mathbf{u}_{3/2}(x, X, y) + \eta^2\mathbf{u}_2(x, X, y) + \cdots \tag{18}$$

$$\lambda - \lambda_c = \eta\lambda_1 + \eta^{3/2}\lambda_{3/2} + \eta^2\lambda_2 + \cdots \tag{19}$$

The orders of magnitude in (13), (14), (18) and (19) have been chosen to be in agreement, first with the expansions of Hunt and Lucena Neto (1991) who do not consider imperfections, second with the result of Koiter (1963) (see also Calladine, 1983), where the double scale analysis is not introduced. Inserting eqns (16)–(19) into the equilibrium eqns (1) and (2), we find equations at the three first orders η, $\eta^{3/2}$, η^2:

$$L_\lambda \mathbf{u}_1 = \mathbf{0} \tag{20}$$

$$L_\lambda \mathbf{u}_{3/2} = \mathbf{F}_{3/2} + \mathbf{G}_l \tag{21}$$

$$L_\lambda \mathbf{u}_2 = \mathbf{F}_2 \tag{22}$$

where

$$L_\lambda = \begin{bmatrix} k^2\Delta^2 + \lambda_c\dfrac{\partial^2}{\partial x^2} & -\rho\dfrac{\partial^2}{\partial x^2} \\ \rho\dfrac{\partial^2}{\partial x^2} & \Delta^2 \end{bmatrix} \tag{23}$$

is the linear operator of the problem, that is the same for the three orders. The right hand sides of (21) and (22) depend on the deflection and stress components: w_i and Φ_i ($i = 1, 3/2$), the expressions of $\mathbf{F}_{3/2}$ and $\mathbf{F}_2$ are given in Appendix A. The vector

$$\mathbf{G}_l = \begin{pmatrix} -\lambda_c \dfrac{\partial^2 g_l(x,y)}{\partial x^2} \\ 0 \end{pmatrix} \tag{24}$$

appearing in eqn (21) accounts for the shape of the localized imperfection.

Following the same idea as in (Hunt and Lucena Neto, 1991), we intend to search the solutions of perturbative eqns (20)–(22), by taking into account interaction modes. In fact, there are many modes that generate the set of solutions of the first order eqn (20). It would be difficult and unnecessary to account for all these modes in the postbuckling analysis. One gets non-linear modal interactions by retaining the axisymmetric mode B and two rectangular modes A and C having the same circumferential wavenumber, as pictured in Fig. 2 (Koiter (1945, 1963)). Note that it is possible to retain only two modes, the axisymmetric one and the square one (case where the modes A and C coincide), see Calladine (1983). Here we retain the solution of the first-order eqn (20) combining three modes:

$$\mathbf{u}_1 = \begin{pmatrix} A(X)\, e^{i\gamma x} \cos\beta\gamma y + B(X)\, e^{i\gamma(1+\beta^2)x} + C(X)\, e^{i\beta^2\gamma x} \cos\beta\gamma y + \text{c.c.} \\ A_1(X)\, e^{i\gamma x} \cos\beta\gamma y + B_1(X)\, e^{i\gamma(1+\beta^2)x} + C_1(X)\, e^{i\beta^2\gamma x} \cos\beta\gamma y + \text{c.c.} \end{pmatrix} \tag{25}$$

where $A_1 = kA$, $B_1 = kB$, $C_1 = kC$. All these modes appear on the Koiter circle, as seen in Fig. 2. Of course, the number of circumferential waves n, in the rectangular modes, must be an integer, i.e. $\beta\gamma = n\rho$. At this stage, the complex amplitudes $A(X)$, $B(X)$ and $C(X)$ are arbitrary functions of the slow variable X because only the rapid variables x and y appear in the differential operator L_λ. With this $\mathbf{u}_1$, the eqn (21) does not contain secular terms and its solution is given by

$$\mathbf{u}_{3/2} = \begin{pmatrix} 0 \\ \mathrm{d}(X)\, e^{i\gamma x} \cos\beta\gamma y + e(X)\, e^{i\gamma(1+\beta^2)x} + f(X)\, e^{i\beta^2\gamma x} \cos\beta\gamma y + \text{c.c.} \end{pmatrix} + \mathbf{u}^l_{3/2} \tag{26}$$

where

$$d(X) = \frac{2ki(1-\beta^2)}{\gamma(1+\beta^2)} A'(X), \quad e(X) = \frac{2ki}{\gamma(1+\beta^2)} B'(X), \quad f(X) = -\frac{2ki(1-\beta^2)}{\gamma\beta^2(1+\beta^2)} C'(X) \tag{27}$$

and where the last term in (26)

$$\mathbf{u}^l_{3/2} = \begin{pmatrix} w^l_{3/2} \\ \Phi^l_{3/2} \end{pmatrix}$$

accounts for the effect of the localized imperfection (we discuss this problem in Section 4). The "prime" in (27) denotes a differentiation with respect to the slow variable X.

The operator L_λ is singular. Hence, the nonhomogeneous eqn (22) has a solution if and only if its right-hand side satisfies the solvability conditions

$$\langle \mathbf{F}_2, \mathbf{v}^*_i \rangle = 0, \quad i = 1, 2, 3 \tag{28}$$

where the vectors $\mathbf{v}^*_i$ $(i = 1, 2, 3)$ belong to the kernel of the adjoint operator L^*_λ. As shown in Appendix B, these solvability conditions yield three coupled non-linear second-order differential

equations for the complex amplitudes $A(X)$, $B(X)$, $C(X)$, which amount to those of Hunt and Lucena Neto (1991) in real case:

$$8k^2(1-\beta^2)^2\frac{\mathrm{d}^2A(X)}{\mathrm{d}X^2}+2\lambda_1 A(X)+6\rho\beta^2 B(X)\bar{C}(X)=0 \tag{29}$$

$$8k^2(1+\beta^2)^2\frac{\mathrm{d}^2B(X)}{\mathrm{d}X^2}+2\lambda_1(1+\beta^2)^2 B(X)+3\rho\beta^2 C(X)A(X)=0 \tag{30}$$

$$8k^2(1-\beta^2)^2\frac{\mathrm{d}^2C(X)}{\mathrm{d}X^2}+2\lambda_1\beta^4 C(X)+6\rho\beta^2\bar{A}(X)B(X)=0 \tag{31}$$

where $(\bar{\ })$ means the complex conjugate of $(\,)$.

Hence eqns (29)–(31) govern the evolution of the modulated complex amplitudes $A(X)$, $B(X)$ and $C(X)$. We show in the next section that, in the presence of localized imperfections, these amplitudes have discontinuous derivatives at $X=0$.

4. Account for local perturbation

We return to the problem (21) where we have seen that the solution which accounts for the localized imperfection satisfies

$$L_\lambda \mathbf{u}^l_{3/2}=\mathbf{G}_l \tag{32}$$

To solve this problem, it is convenient to introduce the Fourier transform defined as

$$\hat{f}(\omega)=\frac{1}{\sqrt{2\pi}}\int_{-\infty}^{+\infty} f(x)\,e^{i\omega x}\,\mathrm{d}x \tag{33}$$

Equation (32) has in general no localized and smooth solution. In their study of a beam buckling problem, Amazigo *et al.* (1970) removed this difficulty by admitting solutions that are discontinuous at $X=0$, what corresponds to the region where the localized imperfection lies. From the point of view of the asymptotic analysis introduced in Section 3, in the presence of a localized imperfection, we solve the non-linear problem by using two different expansions of $\mathbf{u}$ or of their derivatives in the region $x<0$, $X<0$ and in the region $x>0$, $X>0$. Hence any quantity in these asymptotic expansions can admit the possibility of discontinuities at $X=0$, but the unknown $\mathbf{u}$, and its derivative $\mathrm{d}\mathbf{u}/\mathrm{d}x$, $\mathrm{d}^2\mathbf{u}/\mathrm{d}x^2$ and $\mathrm{d}^3\mathbf{u}/\mathrm{d}x^3$ must be continuous at $x=0$ and $X=0$. These continuity conditions lead to conditions on the $\mathbf{u}_n$ and their derivatives (see Appendix C).

Hence, we seek solutions of (32) having discontinuities

$$[f(0)]=f(0^+)-f(0^-) \tag{34}$$

Now the Fourier transform leads to

$$L(\omega)\hat{\mathbf{u}}^l_{3/2}=\mathbf{S}(\omega,y) \tag{35}$$

where

$$L(\omega) = \begin{bmatrix} k^2\left(\omega^2 - \dfrac{\partial^2}{\partial y^2}\right)^2 - \lambda_c\omega^2 & \rho\omega^2 \\ -\rho\omega^2 & \left(\omega^2 - \dfrac{\partial^2}{\partial y^2}\right)^2 \end{bmatrix} \tag{36}$$

is the operator of the problem in the Fourier space. The right hand side $\mathbf{S}(\omega, y)$ of (35) is a complex vector depending on localized imperfections and on the discontinuities of the $\mathbf{u}^l_{3/2}$ and their derivatives at $X = 0$. Its expression is reported in Appendix C.

The operator $L(\omega)$ is singular for $\omega = \gamma$, $\omega = \beta^2\gamma$ and $\omega = \gamma(1+\beta^2)$. Hence, the right hand side of (35) must satisfy the following solvability conditions

$$\langle \mathbf{S}(\omega, y), \mathbf{V}^*_k \rangle = 0, \quad (k = 1, 2, 3) \tag{37}$$

where $\mathbf{V}^*_k$ are the three vectors belonging to the kernel of the adjoint operator $L^*(\omega)$ (see Appendix C).

Finally, in the presence of a localized imperfection, we find that the first order term of the envelopes $A(X)$, $B(X)$ and $C(X)$ are continuous but have discontinuous derivatives at $X = 0$ (i.e. in the region where the localized imperfection is significant) given by the following formulas (the detail of the calculus is reported in Appendix C):

$$[A'(0)] = -\frac{\lambda_c\sqrt{2\pi}}{4k^2\pi R(1-\beta^2)^2}\int_0^{2\pi R} \hat{g}_l(\gamma, y)\cos(\beta\gamma y)\,\mathrm{d}y = \delta_A \tag{38}$$

$$[B'(0)] = -\frac{\lambda_c\sqrt{2\pi}}{8k^2\pi R}\int_0^{2\pi R} \hat{g}_l(\gamma(1+\beta^2), y)\,\mathrm{d}y = \delta_B \tag{39}$$

$$[C'(0)] = -\frac{\lambda_c\beta^4\sqrt{2\pi}}{4k^2\pi R(1-\beta^2)^2}\int_0^{2\pi R} \hat{g}_l(\beta^2\gamma, y)\cos(\beta\gamma y)\,\mathrm{d}y = \delta_C \tag{40}$$

In these equations, $\hat{g}_l(\omega, y)$ is the Fourier transform of $g_l(x, y)$, which represents the shape of the localized imperfection.

Coming back to the unscaled amplitudes and the unscaled variables, we get the following non-linear three coupled second-order differential equations completed by jump relations

$$8k^2(1-\beta^2)^2\frac{\mathrm{d}^2a(x)}{\mathrm{d}x^2} + 2(\lambda-\lambda_c)a(x) + 6\rho\beta^2 b(x)\bar{c}(x) = 0 \tag{41}$$

$$8k^2(1+\beta^2)^2\frac{\mathrm{d}^2b(x)}{\mathrm{d}x^2} + 2(\lambda-\lambda_c)(1+\beta^2)^2 b(x) + 3\rho\beta^2 c(x)a(x) = 0 \tag{42}$$

$$8k^2(1-\beta^2)^2\frac{\mathrm{d}^2c(x)}{\mathrm{d}x^2} + 2(\lambda-\lambda_c)\beta^4\ c(x) + 6\rho\beta^2\bar{a}(x)b(x) = 0 \tag{43}$$

$$\left[\frac{\mathrm{d}a}{\mathrm{d}x}(0)\right] = a_l\delta_A, \quad \left[\frac{\mathrm{d}b}{\mathrm{d}x}(0)\right] = a_l\delta_B, \quad \left[\frac{\mathrm{d}c}{\mathrm{d}x}(0)\right] = a_l\delta_C \tag{44}$$

In what follows, we seek only symmetric solutions with respect to the x-axis. In this case, the amplitudes $a(x)$, $b(x)$ and $c(x)$ are real and verify, on $[0, +\infty[$, the following system and conditions

$$8k^2(1-\beta^2)^2\frac{\mathrm{d}^2a(x)}{\mathrm{d}x^2}+2(\lambda-\lambda_c)a(x)+6\rho\beta^2b(x)c(x)=0 \tag{45}$$

$$8k^2(1+\beta^2)^2\frac{\mathrm{d}^2b(x)}{\mathrm{d}x^2}+2(\lambda-\lambda_c)(1+\beta^2)^2b(x)+3\rho\beta^2c(x)a(x)=0 \tag{46}$$

$$8k^2(1-\beta^2)^2\frac{\mathrm{d}^2c(x)}{\mathrm{d}x^2}+2(\lambda-\lambda_c)\beta^4\ c(x)+6\rho\beta^2a(x)b(x)=0 \tag{47}$$

$$a'(0)=\frac{\delta_A}{2}a_l,\quad b'(0)=\frac{\delta_B}{2}a_l,\quad c'(0)=\frac{\delta_C}{2}a_l \tag{48}$$

Hence eqns (45)–(48) govern the evolution of the amplitudes $a(x)$, $b(x)$, $c(x)$. In the case of a subcritical bifurcation, the localized imperfection transforms the bifurcation point $(\lambda_c, 0, 0, 0)$ into a limit point $(\lambda_{\max}, a_{\max}, b_{\max}, c_{\max})$, $\lambda_{\max}$ being lower than λ_c. The maximal load $\lambda_{\max}$ will be computed by solving the non-linear problem (45)–(47) with the relations (48). We shall propose, in the next section, an analytical formulae giving an estimation of the reduction of the critical load.

5. Reduction of the buckling load

5.1. *Numerical computation of the reduction of the buckling load*

We now compute the reduction of the critical load by solving numerically the amplitude equations and the jump relations. Using a variational formulation of (45)–(48) and a finite element discretization, we get an algebraic non-linear problem in the following classical form:

$$([K_E]-(\lambda-\lambda_c)[K_G]+[K_N])\{\mathbf{u}_n\}=\{d_{abc}\}$$

where $[K_E]$ is an elastic stiffness matrix, $[K_G]$ is a geometrical stiffness matrix, $[K_N]$ is a non-linear stiffness matrix, $\{u_n\}$ is the nodal vector and $\{d_{abc}\}$ is the global vector which depends on the localized imperfection. This problem is solved by a Newton–Raphson algorithm.

Choice of localized imperfection

To solve the problem (45)–(48), we must compute the coefficients, δ_A, δ_B, δ_C, that appear in the jump relations (48) which depend on the Fourier transform of the shape of the localized imperfections. We shall consider an initial imperfection localized around $x=0$, having the following shape:

$$g_l(x,y)=e^{-\left(\frac{x}{C}\right)^2}(d_A\cos\gamma x\cos\beta\gamma y+d_B\cos\gamma(1+\beta^2)x+d_C\cos\gamma\beta^2x\cos\beta\gamma y),\quad C>0 \tag{49}$$

In (49), C is a positive constant which measures the width of the zone where the localized imperfection is significant (Fig. 1(b)) and d_A, d_B, d_C are real numbers. In what follows, they take

only two values 0 or 1. Thus, by choosing $d_A = 1$ and $d_B = d_C = 0$ (or $d_A = d_B = 0$ and $d_C = 1$), we have a localized imperfection on the mode A (or on the mode C). The choice $d_A = d_B = 1$ and $d_C = 0$ (or $d_A = d_B = d_C = 1$) corresponds to a localized imperfection on the two modes A and B (or on the three modes A, B, C). Other choices would be possible. The Fourier transform of (49) is

$$\hat{g}_l(\omega, y) = \frac{C\sqrt{2}}{4}\left[d_A\left(e^{-\left(\frac{(\omega+\gamma)C}{2}\right)^2} + e^{-\left(\frac{(\omega-\gamma)C}{2}\right)^2}\right)\cos\beta\gamma y \right.$$
$$\left. + d_B\left(e^{-\left(\frac{(\omega+\gamma(1+\beta^2))C}{2}\right)^2} + e^{-\left(\frac{(\omega-\gamma(1+\beta^2))C}{2}\right)^2}\right) + d_C\left(e^{-\left(\frac{(\omega+\gamma\beta^2)C}{2}\right)^2} - e^{-\left(\frac{(\omega-\gamma\beta^2)C}{2}\right)^2}\right)\cos\beta\gamma y \right] \quad (50)$$

With this choice, the jump relations (48) become

$$\frac{\mathrm{d}a}{\mathrm{d}x}(0) = -\frac{a_l\lambda_c\sqrt{\pi}C}{16k^2(1-\beta^2)^2}\left[d_A(1+e^{-\gamma^2C^2}) + d_C\left(e^{-\left(\frac{\gamma(1+\beta^2)C}{2}\right)^2} + e^{-\left(\frac{\gamma(1-\beta^2)C}{2}\right)^2}\right)\right] = \frac{\delta_A}{2}a_l \quad (51)$$

$$\frac{\mathrm{d}b}{\mathrm{d}x}(0) = -\frac{a_l\lambda_c\sqrt{\pi}C}{16k^2}[d_B(1+e^{-\gamma(1+\beta^2)C)^2})] = \frac{\delta_B}{2}a_l \quad (52)$$

$$\frac{\mathrm{d}c}{\mathrm{d}x}(0) = -\frac{a_l\lambda_c\sqrt{\pi}C}{16k^2(1-\beta^2)^2}\left[d_A\left(e^{-\left(\frac{\gamma(1+\beta^2)C}{2}\right)^2} + e^{-\left(\frac{\gamma(1-\gamma\beta^2)C}{2}\right)^2}\right) + d_C(1+e^{-\gamma^2\beta^4C^2})\right] = \frac{\delta_C}{2}a_l \quad (53)$$

Let us note that the modal aspect ratio β depends on the number of waves n in the circumferential direction and on the ratio h/R via the following relation

$$\beta = \frac{\sqrt{\frac{R}{k}} \pm \sqrt{\frac{R}{k} - 4n^2}}{2n}, \quad \text{for } n \leqslant \frac{1}{2}\sqrt{\frac{R}{k}} \quad (54)$$

obtained from the required condition (12), where

$$\sqrt{\frac{R}{k}} = \sqrt{\frac{R\sqrt{12(1-\nu^2)}}{h}}$$

This non dimensional parameter β decreases when the wavenumber increases in n. Large modal aspect ratios correspond to small wavenumbers.

We can write the jump relations (51)–(53) as function of n, C/R, h/R and a_l/h by using (11) and the definition of γ:

$$\frac{\mathrm{d}a}{\mathrm{d}x}(0) = \delta_a\frac{a_l}{h}, \quad \frac{\mathrm{d}b}{\mathrm{d}x}(0) = \delta_b\frac{a_l}{h}, \quad \frac{\mathrm{d}c}{\mathrm{d}x}(0) = \delta_c\frac{a_l}{h}$$

where

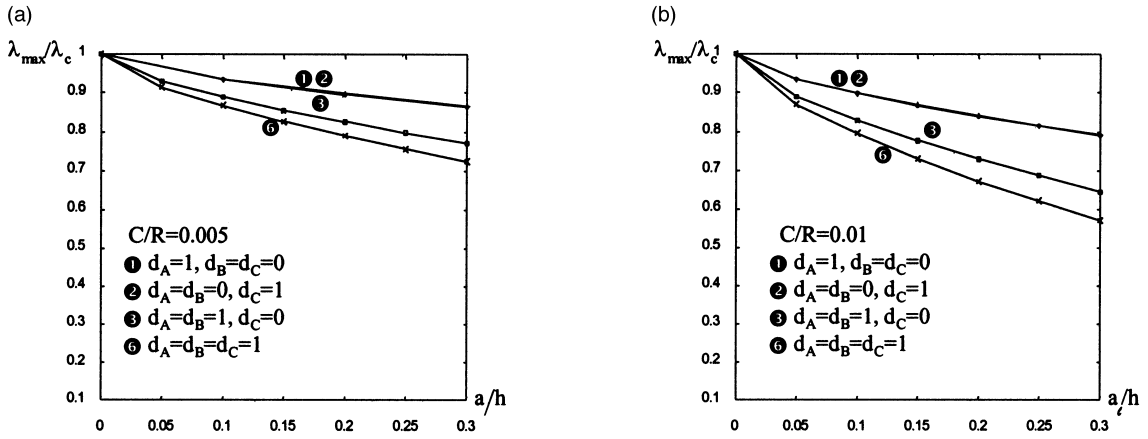

Fig. 3. Numerical reduction of the critical load : $\lambda_{\max}/\lambda_c$ vs a_l/h for $v = 0.3$, $h/R = 0.00247$ and $n = 15$. (a) $C/R = 0.005$. (b) $C/R = 0.01$.

$$\delta_a = -\frac{\sqrt{12\pi(1-v^2)}}{8(1-\beta^2)}\frac{C}{R}\left[d_A\left(1+e^{-\left(\frac{nC}{\beta R}\right)^2}\right)+d_C\left(e^{-\left(\frac{n(1+\beta^2)C}{2\beta R}\right)^2}+e^{-\left(\frac{n(1-\beta^2)C}{2\beta R}\right)^2}\right)\right]$$

$$\delta_b = -\frac{\sqrt{12\pi(1-v^2)}}{8}\frac{C}{R}\left[d_B\left(1+e^{-\left(\frac{n(1+\beta^2)C}{\beta R}\right)^2}\right)\right]$$

$$\delta_c = -\frac{\sqrt{12\pi(1-v^2)}}{8(1-\beta^2)}\frac{C}{R}\left[d_A\left(e^{-\left(\frac{n(1+\beta^2)C}{2\beta R}\right)^2}+e^{-\left(\frac{n(1-\beta^2)C}{2\beta R}\right)^2}\right)+d_C\left(1+e^{-\left(\frac{n\beta C}{R}\right)^2}\right)\right]$$

The non dimensional quantities δ_a, δ_b and δ_c depend only on the ratios h/R, C/R and on n. Remark that these δ_a, δ_b, δ_c are related to the δ_A, δ_B, δ_C defined in (38)–(40) by $\delta_a = \delta_A h/2$, $\delta_b = \delta_B h/2$, $\delta_a = \delta_C h/2$.

The numerical prediction of the reduction of the critical buckling load in the presence of a localized imperfection of amplitude a_l and of width C is presented in Fig. 3. This computation has been carried out by taking the characteristics of the experimental specimens of Yamaki (1984) for which the shell radius $R = 100$ mm, thickness $h = 0.247$ mm and Poisson's ratio $v = 0.3$. We choose a number of waves in the circumferential direction $n = 15$ that gives a mode aspect ratio $\beta \approx 2$. In order to evaluate the effect of the localized imperfection, four different shapes are considered ① $d_A = 1$, $d_B = d_C = 0$, ② $d_A = d_B = 0$, $d_C = 1$, ③ $d_A = d_B = 1$, $d_C = 0$, ⑥ $d_A = d_B = d_C = 1$, for two typical values of C/R ($C/R = 0.005$ and 0.01).

It appears that the reduction of critical load is not proportional to a_l/h, as in the case of a single cellular buckling mode (Amazigo *et al.*, 1970; Damil and Potier-Ferry, 1992). One gets the same reduction, whether the imperfection is on mode A or mode C. As expected, a combination of three modes induces a stronger reduction than a combination of two modes. The ratio C/R has a strong influence on the load carrying capacity of the shell. The Fig. 3 permits us to confirm the high

imperfection sensitivity of this structure because we get 40% of reduction with a very localized imperfection ($C/R = 0.01$) of moderate amplitude ($a_l/h = 0.3$).

In the next paragraph, we show that the reduction is proportional to $(a_l/h)^{2/3}$.

5.2. *Analytic formulae for the reduction of buckling load*

In this section, we propose approximate analytical formulae for the reduction of the critical buckling load. First, let us establish the following proposition.

Proposition: The reduction of the critical buckling load for a cylindrical shell under axial compression, in the presence of a localized imperfection of amplitude a_l is proportional to $(a_l)^{2/3}$:

$$\lambda_{\max} - \lambda_c = O((a_l)^{2/3}) \tag{55}$$

To prove this statement, we introduce a set of new variables ξ, a_1, b_1, c_1 and Λ such that:

$$x = \xi (a_l)^{\mu} \tag{56}$$

$$a = a_1 (a_l)^{\sigma}, \quad b = b_1 (a_l)^{\sigma}, \quad c = c_1 (a_l)^{\sigma} \tag{57}$$

$$\lambda - \lambda_c = \Lambda (a_l)^{\varepsilon} \tag{58}$$

where μ, σ and ε are three exponents which will be determined in the following. Injecting eqns (56)–(58) in (45)–(47), we obtain the scaling form:

$$8k^2(1-\beta^2)^2 \frac{\mathrm{d}^2 a_1}{\mathrm{d}\zeta^2}(a_l)^{-(2\mu+\sigma)} + 2\Lambda a_1 (a_l)^{\varepsilon-\sigma} + 6\rho\beta^2 b_1 c_1 = 0 \tag{59}$$

$$8k^2(1+\beta^2)^2 \frac{\mathrm{d}^2 b_1}{\mathrm{d}\zeta^2}(a_l)^{-(2\mu+\sigma)} + 2(1+\beta^2)^2 \Lambda b_1 (a_l)^{\varepsilon-\sigma} + 3\rho\beta^2 c_1 a_1 = 0 \tag{60}$$

$$8k^2(1-\beta^2)^2 \frac{\mathrm{d}^2 c_1}{\mathrm{d}\zeta^2}(a_l)^{-(2\mu+\sigma)} + 2\beta^4 \Lambda c_1 (a_l)^{\varepsilon-\sigma} + 6\rho\beta^2 a_1 b_1 = 0 \tag{61}$$

The jump relations (48), write under this scaling change as:

$$\frac{\mathrm{d}a_1(0)}{\mathrm{d}\zeta}(a_l)^{\sigma-\mu} = \frac{\delta_A}{2} a_l \tag{62}$$

$$\frac{\mathrm{d}b_1(0)}{\mathrm{d}\zeta}(a_l)^{\sigma-\mu} = \frac{\delta_B}{2} a_l \tag{63}$$

$$\frac{\mathrm{d}c_1(0)}{\mathrm{d}\zeta}(a_l)^{\sigma-\mu} = \frac{\delta_C}{2} a_l \tag{64}$$

The scaling invariance property permits us to calculate this group of components under the considered scaling change. The three non-linear coupled second-order amplitude equations governing the buckling of cylindrical shells must be a scaling invariant. Thus, by comparing eqns (45)–(48) and (59)–(61), we deduce the following relations between components

$$2\mu+\sigma=0,\quad \varepsilon-\sigma=0,\quad \sigma-\mu=1 \tag{65}$$

which gives

$$\sigma=\tfrac{2}{3},\quad \mu=-\tfrac{1}{3},\quad \varepsilon=\tfrac{2}{3} \tag{66}$$

It follows that, the equation (58) can finally be written in the form of power law as:

$$\lambda-\lambda_c=\Lambda(a_l)^{2/3} \tag{67}$$

Hence the reduction of the critical load $\lambda_m-\lambda_c$ is proportional to $(a_l)^{2/3}$.

Reduction formulae for buckling load

We propose here an estimate of the coefficient of proportionality Λ of the reduction formula (67). Based on the conservation of energy, we shall derive an estimated expression of the load in terms of imperfection size, of discontinuities of envelopes and of the cylindrical shell physical characteristics. Indeed, the energy E of the system is (Hunt and Lucena Neto, 1991)

$$E=4k^2\{(1-\beta^2)^2a'^2+2(1+\beta^2)^2b'^2+(1-\beta^2)^2c'^2\}+(\lambda-\lambda_c)(a^2+2(1+\beta^2)^2b^2+\beta^4c^2)+6\rho\beta^2abc \tag{68}$$

The conservation energy principle, and the following boundedness conditions at infinity

$$a(\pm\infty)=\frac{\mathrm{d}a}{\mathrm{d}x}(+\infty)=0,\quad b(\pm\infty)=\frac{\mathrm{d}b}{\mathrm{d}x}(+\infty)=0,\quad c(+\infty)=\frac{\mathrm{d}c}{\mathrm{d}x}(\pm\infty)=0 \tag{69}$$

give $(E(\infty)-E(0)=0)$

$$0=4k^2\{(1-\beta^2)^2a'^2(0)+2(1+\beta^2)^2b'^2(0)+(1-\beta^2)^2c'^2(0)\}+(\lambda-\lambda_c)(a^2(0)+2(1+\beta^2)^2b^2(0)+\beta^4c^2(0))+6\rho\beta^2a(0)b(0)c(0) \tag{70}$$

For this expression one can get a relation between the load λ and the amplitude of the imperfection:

$$\lambda=\lambda_c-\frac{k^2(1-\beta^2)^2(\delta_A^2+\delta_C^2)+2k^2(1+\beta^2)^2\delta_B^2}{a^2(0)+2(1+\beta^2)^2b^2(0)+\beta^4c^2(0)}a_l^2-6\rho\beta^2\frac{a(0)b(0)c(0)}{a^2(0)+2(1+\beta^2)^2b^2(0)+\beta^4c^2(0)} \tag{71}$$

The quantities $a(0)$, $b(0)$, $c(0)$ depend on the load by eqns (45)–(48). The critical load is the maximum of λ along this solution path. We propose here to forget the basic eqns (45)–(48) and we try to maximize the parameter given by eqn (71) with respect to displacement measures $a(0)$, $b(0)$ and $c(0)$, respectively, namely

$$\frac{\partial\lambda}{\partial a(0)}=0,\quad \frac{\partial\lambda}{\partial b(0)}=0,\quad \frac{\partial\lambda}{\partial c(0)}=0 \tag{72}$$

So we get an approximation of the critical load. (A detailed computation is reported in Appendix D).

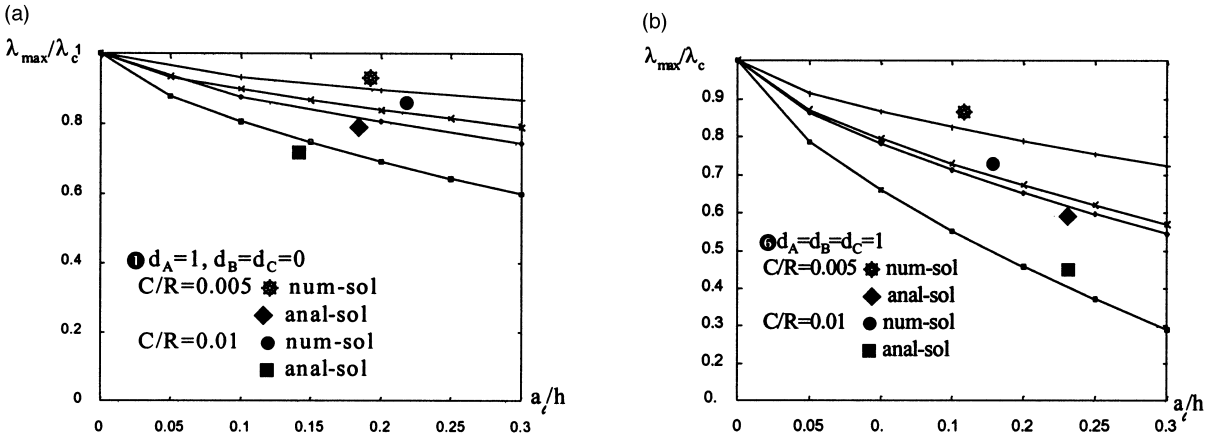

Fig. 4. Comparison between numerical (45)–(47), (51)–(53) and analytical results (73) for the reduction of the critical load for $v = 0.3$, $h/R = 0.00247$, $C/R = 0.005$, 0.01 and $n = 15$. (a) Shape ①: $d_A = 1$, $d_B = d_C = 0$. (b) Shape ⑥: $d_A = d_B = d_C = 1$.

$$\frac{\lambda_{\max}}{\lambda_c} = 1 - F\left(\frac{h}{R}, \frac{C}{R}, n\right)\left(\frac{a_l}{h}\right)^{2/3} \tag{73}$$

where

$$F\left(\frac{h}{R}, \frac{C}{R}, n\right) = \frac{1}{\lambda_c^{1/3}}\left(\frac{9((1-\beta^2)^2(\delta_a^2+\delta_c^2)+2(1+\beta^2)^2\delta_b^2)}{8(1+\beta^2)^2}\right)^{1/3} \tag{74}$$

is the function of proportionality of the reduction of the critical load.

A correction of the reduction formula

Comparing the predicted (73) and calculated results (Fig. 4), we remark that the approximate analytic formula (73) subestimates the reduction of critical load. Obviously, this difference is due to the approximation made to derive (73) from (71). An exact expression of the buckling load $\lambda(a, b, c)$ should be rigorously extracted from the non-linear system (45)–(48), but the coupling and the non-linear character of equations make difficult viz impossible this analytical extraction.

Nevertheless, this approximate analytic formula can give a better estimation of the reduction of the critical load if we correct the proportionality coefficient $F(h/R, C/R, n)$ in (73). In order to examine the difference between the two results, we have computed the ratio $C(h/R, C/R, n)$ between the numerical value of the proportionality coefficient

$$F_{\text{numerical}}\left(\frac{h}{R}, \frac{C}{R}, n\right) = \frac{1 - \dfrac{\lambda_{\max}^{\text{numerical}}}{\lambda_c}}{\left(\dfrac{a_l}{h}\right)^{2/3}}$$

and the analytical one (74) for several tests.

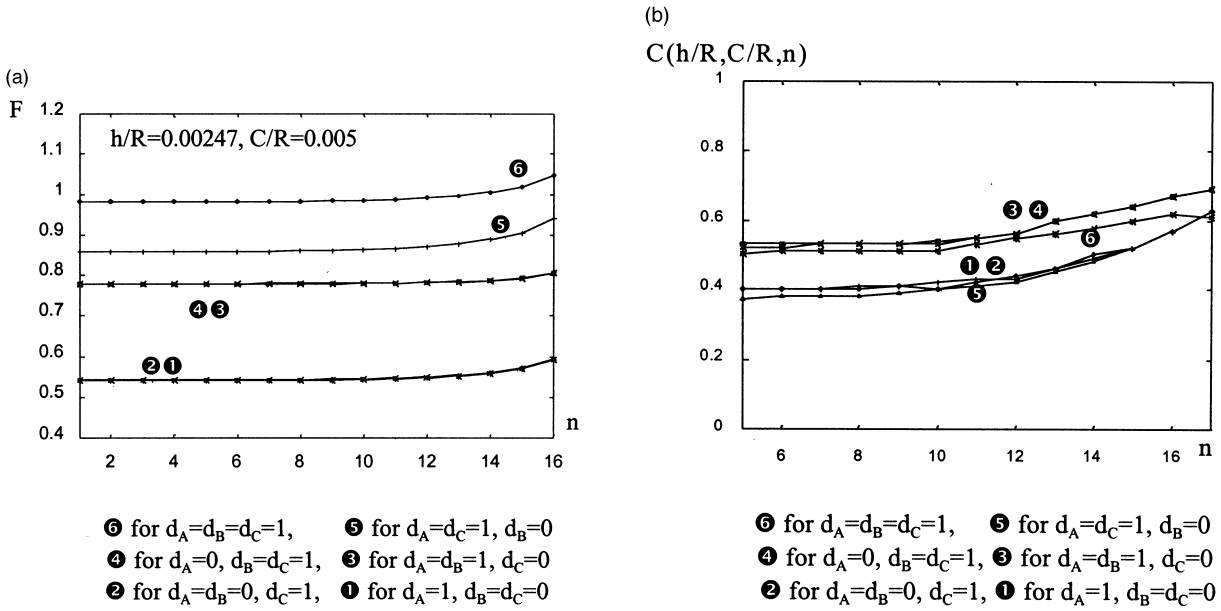

Fig. 5. (a) Variation of the analytical proportionality coefficient $F(73)$ with the number n. Six cases of shapes of localized imperfections. $h/R = 0.00247$ and $C/R = 0.005$, 0.01. (b) Variation of the ratio $C(h/R, C/R, n)$ with the number n. Six cases of shapes of localized imperfections. $h/R = 0.00247$ and $C/R = 0.005$, 0.01.

Let us note that the ratio $C(h/R, C/R, n)$ depends strongly both on the shape of localized imperfections and on the parameters h/R, n and C/R. To study its variation, we have carried out several tests by choosing different shapes of imperfections and varying h/R, n and also C/R. Six shapes of imperfections have been considered: a defect on one mode (only the mode A ① or the mode C ②), a defect on two modes (A and B ③ , A and C ④ , B and C ⑤), a defect on the three modes (A, B and C ⑥).

Let us remark that the analytical proportionality coefficient F eqn. (74) do not depend strongly on the wavenumber n for a fixed shape of defect as it can be seen on Fig. 5a, while the numerical one $F_{\text{numerical}}$ depends slowly on the wave number n. In Fig. 5b, we have plotted the ratio $C(h/R, C/R, n)$ of the two proportionality coefficients for fixed values of h/R and C/R vs n for the six shapes of defect. One can remark that there are two families of curves. The first one corresponds to vanishing axisymmetric localized defect $d_B = 0$ and the second to non vanishing axisymmetric localized defect $d_B = 1$. We have remarked, for the considered set of shapes of the localized imperfection, that the value of the ratio $C(h/R, C/R, n)$ cover the range: $0.35 \leqslant C(h/R, C/R, n) \leqslant 0.57$, for the first family and cover the range: $0.48 \leqslant C(h/R, C/R, n) \leqslant 0.67$, for the second family as is shown in Fig. 5b.

Analysing the results of these tests, we propose the correction $F_{\text{COR}}(h/R, C/R, n)$ of the proportionality coefficient that would be able to reproduce the numerical result for the considered six shapes with a small difference in the presence of an axisymmetric imperfection

$$F_{\text{COR}}\left(\frac{h}{R}, \frac{C}{R}, n\right) = \frac{1}{\lambda_c^{1/3}} \left(\frac{9(C_{\text{COR}1}(1-\beta^2)^2(\delta_a^2+\delta_c^2) + C_{\text{COR}2}(1+\beta^2)^2\delta_b^2)}{8(1+\beta^2)^2} \right)^{1/3} \tag{75}$$

Then the corrected approximate analytic formulae (73) will become

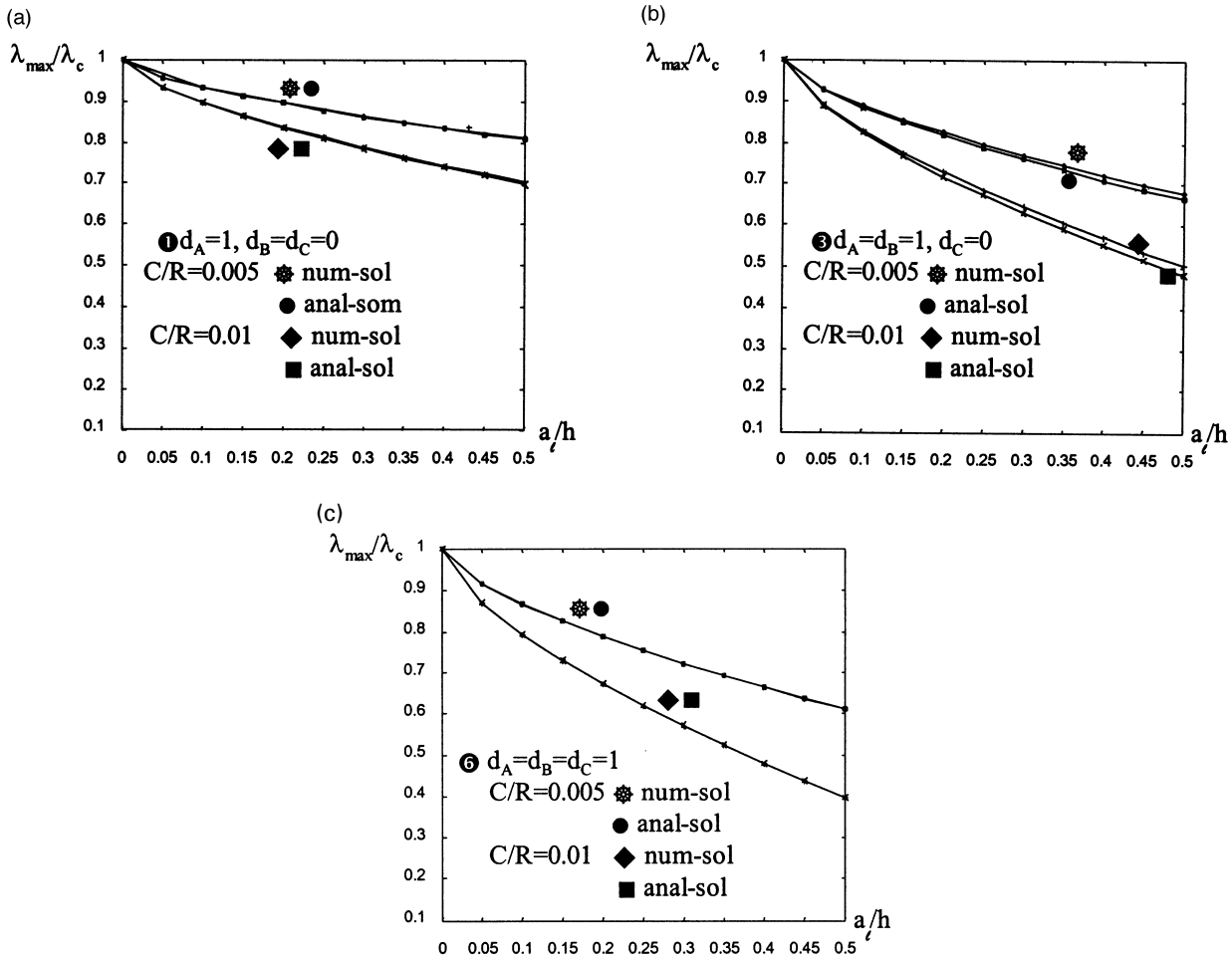

Fig. 6. Comparison between numerical results (45)–(47), (51)–(53) and corrected analytical formulae (76) for the reduction of the critical load for $\nu = 0.3$, $h/R = 0.00247$, $C/R = 0.005$, 0.01 and $n = 15$. $C_{\mathrm{COR1}} = 0.14$, $C_{\mathrm{COR2}} = 0.8$: (a) Shape ①: $d_A = 1$, $d_B = d_C = 0$; (b) Shape ③: $d_A = d_B = 1$, $d_C = 0$; (c) Shape ⑥: $d_A = d_B = d_C = 1$.

$$\frac{\lambda_{\max}}{\lambda_c} = 1 - F_{\mathrm{COR}}\left(\frac{h}{R}, \frac{C}{R}, n\right)\left(\frac{a_l}{h}\right)^{2/3} \tag{76}$$

Let us remark, that correction-factors C_{COR1}, C_{COR2} depend weakly on C/R at fixed values of n and h/R for the six shapes.

By comparing (75) with many numerical results we have found the best values of the correction-factors $C_{\mathrm{COR1}} = 0.14$, $C_{\mathrm{COR2}} = 0.8$. These correction-factors have been chosen to fit the exact values in the range of the largest wavenumbers ($14 < n < 18$), that are generally observed in experiments (see Yamaki, 1984).

Some comparison between the corrected analytic formulae (76), (75) with $C_{\mathrm{COR1}} = 0.14$, $C_{\mathrm{COR2}} = 0.8$ and the numerical result are plotted in Fig. 6 for the three cases of the shapes of the

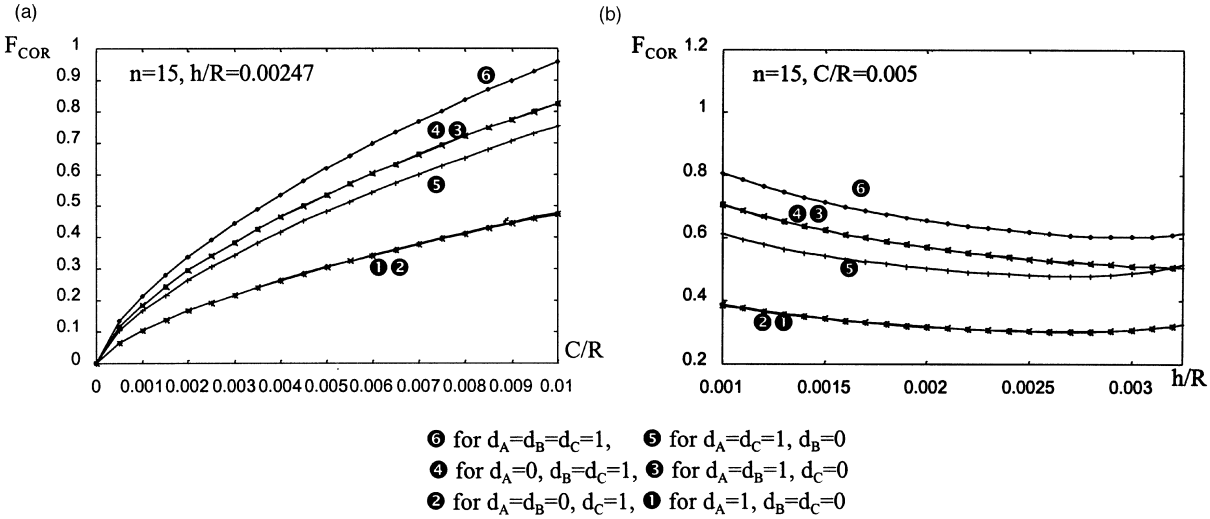

Fig. 7. Variation of the corrected proportionality coefficient F_{COR} (75) for the six cases of shapes of localized imperfections. (a) With the ratio C/R, $h/R = 0.00247$, $n = 15$. (b) With the ratio h/R, $n = 15$ and $C/R = 0.005$, 0.01.

localized imperfection ① , ③ , ⑥ with $n = 15$ and C/R fixed at 0.005 and 0.01. In Fig. 6 the ratio a_l/h takes values until 0.5, while in Figs 3 and 4 its value is limited to 0.3. We see that the two results are in a good agreement for all shapes of the localized imperfection considered.

The eqns (76), (75) give explicitly an approximated relation between the maximal load and the localized imperfection. The variation of the proportionality coefficient $F_{COR}(h/R, C/R, n)$ in eqn (75) as a function of the ratios C/R (width/radius), h/R (thickness/radius) is reported in Fig. 7(a) and 7(b), respectively, for the six shapes ①–⑥ . These plots show that for $n = 15$ and $h/R = 0.00247$, F_{COR} strongly increases with the increase in C/R while for C/R and n fixed F_{COR} is a decreasing function of h/R in interval [0.001, 0.003].

In summary, the reduction of load carrying capacity depends mainly on the size and on the shape of imperfection, via several non dimensional parameters C/R, h/R, n, a_l/h, d_A, d_B, d_C. Our asymptotic analysis predicts a reduction of critical load proportional to $(a_l/h)^{2/3}$, while generally localized imperfections lead to a reduction proportional to a_l/h. As expected, that reduction is greater if the imperfection combines two or three modes. The amplitude a_l/h and the width of imperfection C/R are the main parameters. The shell geometry has a weak influence via the ratio h/R (see Fig. 7(b)), but above all the shell geometry determined the possible modes and the critical load λ_c. Because the present analysis is asymptotic, it is only valid for rather small values of a_l/h and C/R. To determine the range of validity of the present results, a complete numerical solution of the Donnell equations would be necessary, that has not been done in this work.

6. Conclusion

In this paper, we have analysed in the framework of the cellular bifurcation theory the influence of localized imperfections on the buckling of a long cylindrical shell subjected to an axial

compression. Using a double scale perturbation technique, including interaction between three modes, we have established, that the modulated amplitudes are governed by three coupled non-linear differential equations with discontinuous derivatives in the region where the localized imperfections are significant. According to these equations, the reduction of buckling critical load is proportional to $(a_l)^{2/3}$, where a_l is the amplitude of the localized imperfection. A corrected analytical formula, eqn (76), for the reduction of critical load due to localized imperfection has been derived.

Appendix A: Component expressions of vectors $\mathbf{F}_{3/2}$ and $\mathbf{F}_2$

In this Appendix, we give the components of the vectors $\mathbf{F}_{3/2}$ and $\mathbf{F}_2$ appearing in the right hand side of problems (21) and (22), of Section 3.

For the determination of $\mathbf{F}_{3/2}$ and $\mathbf{F}_2$, we substitute the operational rules (16), (17) and the series expansion (18), (19) into equilibrium eqns (1) and (2). This gives the following expressions

$$\mathbf{F}_{3/2} = \begin{pmatrix} f_{3/2,1} \\ f_{3/2,2} \end{pmatrix} = \begin{pmatrix} -2\dfrac{\partial^2}{\partial x\,\partial X}((2k^2\Delta+\lambda_c)w_1-\rho\Phi_1) \\ -2\dfrac{\partial^2}{\partial x\,\partial X}(\rho w_1+2\Delta\Phi_1) \end{pmatrix} \tag{A1}$$

and

$$\mathbf{F}_2 = \begin{pmatrix} f_{2,1} \\ f_{2,2} \end{pmatrix}$$

with

$$\begin{aligned} f_{2,1} &= -\lambda_1\frac{\partial^2 w_1}{\partial x^2} - 2\frac{\partial^2}{\partial x\,\partial X}(2k^2\Delta+\lambda_c)w_{3/2} + \rho\left(\frac{\partial^2\Phi}{\partial X^2}+2\frac{\partial^2\Phi_{3/2}}{\partial x\,\partial X}\right) \\ &\quad -\left(4k^2\frac{\partial^4}{\partial x^2\,\partial X^2}+\frac{\partial^2}{\partial X^2}(2\Delta+\lambda_c)\right)w_1+[w_1,\Phi_1] \\ f_{2,2} &= -4\frac{\partial^2}{\partial x\,\partial X}\Delta\Phi_{3/2}-\rho\left(\frac{\partial^2 w_1}{\partial X^2}+2\frac{\partial^2 w_{3/2}}{\partial x\,\partial X}\right)-2\frac{\partial^2}{\partial X^2}\left(2\frac{\partial^2}{\partial x^2}+\Delta\right)\Phi_1-\frac{1}{2}[w_1,w_1] \end{aligned} \tag{A2}$$

where (w_1,Φ_1) and $(w_{3/2},\Phi_{3/2})$ are, respectively, the solutions of linear problems (20) and (21) given by (25) and (26) without localized imperfections. We recall here that the bracket operator [,] is defined by eqn (4) of Section 2.

Appendix B: Derivation of the three coupled amplitude equations

The problem (22) will have a bounded solution if and only if it satisfies to the following solvability conditions:

$$\langle \mathbf{F}_2, \mathbf{v}_i^* \rangle = 0, \quad i = 1,2,3 \tag{B1}$$

where the three vectors $\mathbf{v}_i^*$ belonging to the kernel of the adjoint operator L_λ^* of L_λ are given by

$$\mathbf{v}_1^* = \begin{pmatrix} e^{-i\gamma x}\cos\beta\gamma y \\ -ke^{-i\gamma x}\cos\beta\gamma y \end{pmatrix}, \quad \mathbf{v}_2^* = \begin{pmatrix} e^{-i\gamma(1+\beta^2)x} \\ -ke^{-i\gamma(1+\beta^2)x} \end{pmatrix}, \quad \mathbf{v}_3^* = \begin{pmatrix} e^{-i\gamma\beta^2 x}\cos\beta\gamma y \\ -ke^{-i\gamma\beta^2 x}\cos\beta\gamma y \end{pmatrix} \tag{B2}$$

The mean value in (B1) is defined by:

$$\langle f(x,y), g(x,y) \rangle = \lim_{M\to+\infty} \frac{1}{M} \int_{-M}^{M} \int_{0}^{2\pi R} f(x,y) g(x,y)\, \mathrm{d}y\, \mathrm{d}x \tag{B3}$$

The solvability conditions (28) are equivalent to

$$\begin{aligned}
\langle \mathbf{F}_2, \mathbf{v}_1^* \rangle &= \lim_{M\to+\infty} \frac{1}{M} \int_{-M}^{+M} \int_{0}^{2\pi R} (f_{2,1} - k f_{2,2})\, e^{-i\gamma x} \cos(\beta\gamma y)\, \mathrm{d}y\, \mathrm{d}x = 0 \\
\langle \mathbf{F}_2, \mathbf{v}_2^* \rangle &= \lim_{M\to+\infty} \frac{1}{M} \int_{-M}^{+M} \int_{0}^{2\pi R} (f_{2,1} - k f_{2,2})\, e^{-i\gamma(1+\beta^2)x}\, \mathrm{d}y\, \mathrm{d}x = 0 \\
\langle \mathbf{F}_2, \mathbf{v}_3^* \rangle &= \lim_{M\to+\infty} \frac{1}{M} \int_{-M}^{+M} \int_{0}^{2\pi R} (f_{2,1} - k f_{2,2})\, e^{-i\gamma\beta^2 x} \cos(\beta\gamma y)\, \mathrm{d}y\, \mathrm{d}x = 0
\end{aligned} \tag{B4}$$

where $f_{2,1}$ and $f_{2,2}$ are given by (A2) (see Appendix A). Therefore, by taking (25), (26) without localized solution $\mathbf{u}_{3/2}^l$ and (27), we obtain, after performing integrations in (B4), three coupled non-linear second order differential equations given by (29)–(31).

Appendix C: Computation of the discontinuities of first derivatives of amplitudes

We report in this Appendix the details of computation permitting to get the first derivative discontinuities of amplitudes $A(X)$, $B(X)$ and $C(X)$ at $X = 0$.

In Section 4, we have noted that to solve problem (32) which account for localized imperfections, it is convenient to introduce the Fourier transform defined by (33) and to seek a solution of (32) having discontinuities

$$[f(0)] = f(0^+) - f(0^-) \tag{C1}$$

This leads to the problem

$$L(\omega)\mathbf{u}^{\hat{I}}_{3/2} = \mathbf{S}(\omega, y) \tag{C2}$$

where the components $S_1(\omega, y)$ and $S_2(\omega, y)$ of $\mathbf{S}(\omega, y)$ are expressed in the terms of the possible discontinuities of $\mathbf{u}_{3/2}$ and its derivatives as follows

$$\begin{aligned}
S_1(\omega, y) = \frac{1}{\sqrt{2\pi}}\Bigg(& k^2\left[\frac{\partial^3 w^I_{3/2}}{\partial x^3}(0, y)\right] - i\omega k^2\left[\frac{\partial^2 w^I_{3/2}}{\partial x^2}(0, y)\right] - k^2\omega^2\left[\frac{\partial w^I_{3/2}}{\partial x}(0, y)\right] + i\omega^3 k^2[w^I_{3/2}(0, y)] \\
& + 2k^2\left[\frac{\partial^3 w^I_{3/2}}{\partial y^2\,\partial x}(0, y)\right] - 2i\omega k^2\left[\frac{\partial^2 w^I_{3/2}}{\partial y^2}(0, y)\right] + \lambda_c\left[\frac{\partial w^I_{3/2}}{\partial x}(0, y)\right] - i\lambda_c\omega[w^I_{3/2}(0, y)] \\
& - \rho\left[\frac{\partial \Phi^I_{3/2}}{\partial x}(0, y)\right] + i\rho\omega[\Phi^I_{3/2}(0, y)] + \lambda_c\left[\frac{\partial g_I}{\partial x}(0, y)\right] - i\lambda_c\omega[g_I(0, y)]\Bigg) + \lambda_c\omega^2\hat{g}_I(\omega, y) \\
S_2(\omega, y) = \frac{1}{\sqrt{2\pi}}\Bigg(& \left[\frac{\partial^3 \Phi^I_{3/2}}{\partial x^3}(0, y)\right] - i\omega\left[\frac{\partial^2 \Phi^I_{3/2}}{\partial x^2}(0, y)\right] - \omega^2\left[\frac{\partial \Phi^I_{3/2}}{\partial x}(0, y)\right] + i\omega^3[\Phi^I_{3/2}(0, y)] \\
& + 2\left[\frac{\partial^3 \Phi^I_{3/2}}{\partial y^2\,\partial x}(0, y)\right] - 2i\omega\left[\frac{\partial^2 \Phi^I_{3/2}}{\partial y^2}(0, y)\right] + \rho\left[\frac{\partial w^I_{3/2}}{\partial x}(0, y)\right] - i\rho\omega[w^I_{3/2}(0, y)]\Bigg)
\end{aligned} \tag{C3}$$

We admit the possibility of discontinuity in the $\mathbf{u}_i$'s and in their derivatives at $x = 0$ and $X = 0$, as in (Amazigo *et al.*, 1970; Damil and Potier-Ferry, 1992), but the generalized deflection $\mathbf{u}$, the generalized slope $\mathrm{d}\mathbf{u}/\mathrm{d}x$, the generalized moment $\mathrm{d}^2\mathbf{u}/\mathrm{d}x^2$ and the generalized shear $\mathrm{d}^3\mathbf{u}/\mathrm{d}x^3$ must be continuous in x and X. These continuity conditions lead to the following continuity conditions on the $\mathbf{u}_n$ and their derivatives.

$$\left\{\begin{array}{c}
\mathbf{u}_i \\
\dfrac{\partial \mathbf{u}_i}{\partial x} + \dfrac{\partial \mathbf{u}_{i-1/2}}{\partial X} \\
\dfrac{\partial^2 \mathbf{u}_i}{\partial x^2} + 2\dfrac{\partial^2 \mathbf{u}_{i-1/2}}{\partial x\,\partial X} + \dfrac{\partial^2 \mathbf{u}_{i-1}}{\partial X^2} \\
\dfrac{\partial^3 \mathbf{u}_i}{\partial^3 x} + 3\dfrac{\partial^3 \mathbf{u}_{i-1/2}}{\partial x^2\,\partial X} + 3\dfrac{\partial^3 \mathbf{u}_{i-1}}{\partial x\,\partial X^2} + \dfrac{\partial^3 \mathbf{u}_{i-3/2}}{\partial X^2}
\end{array}\right. \quad \text{are continuous at } x = X = 0 \tag{C4}$$

It is understood in (C4) that $\mathbf{u}_k = 0$ for $k < 1$. It should be noted here that the shape of localized imperfection and their derivatives are continuous. The continuity of the generalized displacement at $x = 0$ and $X = 0$, which permits us to express the discontinuity of (w^I_i, Φ^I_i) and their derivatives as functions of the real and imaginary parts of the jumps in first derivatives of amplitudes $[A'(0)]$, $[B'(0)]$ and $[C'(0)]$.

$$[w^I_{3/2}(0, y)] = 0$$

$$[\Phi^{I}_{3/2}(0,y)] = \frac{4k(1-\beta^2)}{\gamma(1+\beta^2)\sqrt{2\pi}}\left([\mathrm{Im}\,A'(0)] - \frac{1}{\beta^2}[\mathrm{Re}\,C'(0)]\right)\cos\beta\gamma y + \frac{4k}{\gamma(1+\beta^2)}[\mathrm{Im}\,B'(0)]$$

$$\left[\frac{\partial w^{I}_{3/2}}{\partial x}(0,y)\right] = -2[\mathrm{Re}\,A'(0)]\cos\beta\gamma y - 2[\mathrm{Re}\,B'(0)] - 2[\mathrm{Re}\,C'(0)]\cos\beta\gamma y$$

$$\left[\frac{\partial \Phi^{I}_{3/2}}{\partial x}(0,y)\right] = \left(\frac{2k(1-3\beta^2)}{(1+\beta^2)}[\mathrm{Re}\,A'(0)] - \frac{2k(3-\beta^2)}{(1+\beta^2)}[\mathrm{Re}\,C'(0)]\right)\cos\beta\gamma y + 2k[\mathrm{Re}\,B'(0)]$$

$$\left[\frac{\partial^2 w^{I}_{3/2}}{\partial x^2}(0,y)\right] = 4\gamma[\mathrm{Im}\,A'(0)]\cos\beta\gamma y + 4\gamma(1+\beta^2)[\mathrm{Im}\,B'(0)] + 4\gamma\beta^2[\mathrm{Im}\,C'(0)]\cos\beta\gamma y$$

$$\left[\frac{\partial^2 \Phi^{I}_{3/2}}{\partial x^2}(0,y)\right] = \frac{8k\gamma\beta^2}{(1+\beta^2)}[\mathrm{Im}\,A'(0)]\cos\beta\gamma y + \frac{8k\gamma\beta^2}{(1+\beta^2)}[\mathrm{Im}\,C'(0)]\cos\beta\gamma y$$

$$\left[\frac{\partial^3 w^{I}_{3/2}}{\partial x^3}(0,y)\right] = 6\gamma^2[\mathrm{Re}\,A'(0)]\cos\beta\gamma y + 6\gamma^2(1+\beta^2)[\mathrm{Re}\,B'(0)] + 6\gamma^2\beta^4[\mathrm{Re}\,C'(0)]\cos\beta\gamma y$$

$$\left[\frac{\partial^3 \Phi^{I}_{3/2}}{\partial x^3}(0,y)\right] = \left(\frac{2k\gamma^2(1+5\beta^2)}{(1+\beta^2)}[\mathrm{Re}\,A'(0)] + \frac{2k\gamma^2\beta^4(5+\beta^2)}{(1+\beta^2)}[\mathrm{Re}\,C'(0)]\right)\cos\beta\gamma y + 2k\gamma^2(1+\beta^2)[\mathrm{Re}\,B'(0)] \tag{C5}$$

where the symbols Re(...) and Im(...) are the real and the imaginary parts, respectively, of (...). Reporting the relations (C5) into (C3) by taking into account the continuity of the localized imperfection and its first derivative at $x = 0$, we get

$$S_1(\omega,y) = \lambda_c\omega^2\hat{g}_I(\omega,y) + \frac{1}{\sqrt{2\pi}}\left(2k^2(\omega^2+\gamma^2\beta^4)[\mathrm{Re}\,A'(0)]\cos\beta\gamma y + 2k^2\omega^2[\mathrm{Re}\,B'(0)] + 2k^2(\omega^2+\gamma^2)[\mathrm{Re}\,C'(0)]\cos\beta\gamma y - \frac{i4k^2\omega\gamma}{\beta^2}(\beta^6[\mathrm{Im}\,A'(0)] + [\mathrm{Im}\,C'(0)])\cos\beta\gamma y\right)$$

$$S_2(\omega,y) = \frac{1}{\sqrt{2\pi}}\left(\frac{2k}{1+\beta^2}(\beta^4\gamma^2(3-\beta^2) - \omega^2(1-3\beta^2))[\mathrm{Re}\,A'(0)]\cos\beta\gamma y - 2k\omega^2[\mathrm{Re}\,B'(0)] + \frac{2k}{1+\beta^2}(\omega^2(3-\beta^2) - \gamma^2(1-3\beta^2))[\mathrm{Re}\,C'(0)]\cos\beta\gamma y + \frac{i4k\omega^3}{\gamma(1+\beta^2)}[\mathrm{Im}\,B'(0)] + \frac{i4k\omega}{\gamma(1+\beta^2)}((\omega^2(1-\beta^2) - 2\beta^4\gamma^2)[\mathrm{Im}\,A'(0)])\cos\beta\gamma y - \frac{i4k\omega}{\gamma(1+\beta^2)}\left(\frac{1}{\beta^2}(2\beta^2\gamma^2 + \omega^2(1-\beta^2))[\mathrm{Im}\,C'(0)]\right)\cos\beta\gamma y\right) \tag{C6}$$

Since, the operator $L(\omega)$ is singular for $\omega = \gamma$, $\omega = \beta^2\gamma$ and $\omega = \gamma(1+\beta^2)$, then the eqn (C2) has a solution if and only if its right-hand side satisfies the solvability conditions

$$\langle \mathbf{S}(\omega, y), \mathbf{V}_k^* \rangle = 0, \quad (k = 1, 2, 3) \tag{C7}$$

where

$$L^*(\omega = \gamma)\mathbf{V}_1^* = 0, \quad L^*(\omega = \gamma(1+\beta^2))\mathbf{V}_2^* = 0, \quad L^*(\omega = \beta^2\gamma)\mathbf{V}_3^* = 0 \tag{C8}$$

with $L^*(\omega)$ is the adjoint operator of $L(\omega)$, which is not self-adjoint and whose kernel is generated by the vector $\mathbf{V}_k^*$ given by

$$\mathbf{V}_1^* = \mathbf{V}_3^* = \begin{pmatrix} \cos\beta\gamma y \\ -k\cos\beta\gamma y \end{pmatrix}, \quad \mathbf{V}_2^* = \begin{pmatrix} 1 \\ -k \end{pmatrix} \tag{C9}$$

The scalar product in (37) is defined by:

$$\langle f(y), v(y) \rangle = \int_0^{2\pi R} f(y)v(y)\,\mathrm{d}y \tag{C10}$$

(C7) and (C10) give

$$\begin{aligned} &\int_0^{2\pi R} (S_1(\gamma, y) - kS_2(\gamma, y))\cos(\beta\gamma y)\,\mathrm{d}y = 0 \\ &\int_0^{2\pi R} (S_1(\gamma(1+\beta^2), y) - kS_2(\gamma(1+\beta^2), y))\,\mathrm{d}y = 0 \\ &\int_0^{2\pi R} (S_1(\beta^2\gamma, y) - kS_2(\beta^2\gamma, y))\cos(\beta\gamma y)\,\mathrm{d}y = 0 \end{aligned} \tag{C11}$$

The calculus of these integrals gives the expressions (38)–(40) of jumps in first derivatives of amplitudes at $X = 0$.

Appendix D: Reduction formulae for buckling load

To simplify the writing, we introduce the following notations

$$\begin{aligned} &a(0) = \sigma_1, \quad b(0) = \sigma_2, \quad c(0) = \sigma_3 \\ &\chi = \sigma_1^2 + 2(1+\beta^2)^2\sigma_2^2 + \beta^4\sigma_3^2 \\ &\tau = \sigma_1\sigma_2\sigma_3, \quad r = 6\rho\beta^2 \\ &\theta = k^2[(1-\beta^2)^2(\delta_A^2 + \delta_C^2) + 2(1+\beta^2)^2\delta_B^2] \end{aligned} \tag{D1}$$

So, the eqns (D1) give, after multiplication of the three equations obtained from (71) and (72), respectively, by σ_1, σ_2 and σ_3, the following system where the unknown variables χ and τ are

$$r\chi\tau - 2\sigma_1^2(\theta a_l^2 + r\tau) = 0 \tag{D2}$$

$$r\chi\tau - 4(1+\beta^2)^2\sigma_2^2(\theta a_l^2 + r\tau) = 0 \tag{D3}$$

$$r\chi\tau - 2\beta^4\sigma_3^2(\theta a_l^2 + r\tau) = 0 \tag{D4}$$

Its solution is obtained by adding (respectively multiplying) the previous eqns (D2)–(D4), which is

$$\chi = 6\left(\frac{\beta^2(1+\beta^2)\theta}{r}\right)^{2/3} a_l^{4/3} \tag{D5}$$

$$\tau = \frac{2\theta}{r}a_l^2 \tag{D6}$$

Inserting (D5) and (D6) in (65) written in terms of χ and τ as follows,

$$\lambda = \lambda_c - \frac{1}{\chi}(\theta a_l^2 + r\tau) \tag{D7}$$

we obtain the maximal load parameter given by eqn (67).

References

Abdelmoula, R., Damil, N., Potier-Ferry, M., 1992. Influence of distributed and localized imperfections on the buckling of cylindrical shells. International Journal of Solids and Structures 29, 1–25.

Amazigo, J.C., Budiansky, B., Carrier, G.F., 1970. Asymptotic analyses of the buckling of imperfect columns on non-linear elastic foundations. International Journal of Solids and Structures 6, 1341–1356.

Amazigo, J.C,. Fraser, W.B., 1971. Buckling under external pressure of cylindrical shells with dimple shaped initial imperfection. International Journal of Solids and Structures 7, 883–900.

Arbocz, J. et al., 1987. Buckling and post-buckling behaviour of elastic structures. Lecture Notes in Physics. Springer Verlag, Heidelberg.

Brush, D.O., Almroth, B.O., 1975. Buckling of Bars, Plates and Shells. McGraw-Hill, New York.

Bushnell, D., 1985. Computerized Buckling Analysis of Shells. Martinus Nijhoff Publishers Group.

Calladine, C.R., 1983. Theory of Shell Structures. Cambridge University Press, Cambridge.

Combescure, A., 1995. Stability of thin shells of revolution (in French). Thèse d'habilitation à diriger des recherches, INSA de Lyon.

Damil, N., Potier-Ferry, M. 1986. Wavelength selection in the postbuckling of a long rectangular plate. International Journal of Solids and Structures 22, 511–526.

Damil, N., Potier-Ferry, M., 1992. Amplitude equations for cellular instability. Dynamics and Stability of Systems 7, 1–35.

Hunt, G.W., Lucena Neto, 1991. Localized buckling in long axially-loaded cylindrical shells. Journal of the Mechanics and Physics of Solids 39(7), 881–894.

Koiter, W.T., 1945. On the stability of elastic equilibrium. Ph.D. thesis, Delft. English translation, NASA Techn. Trans. F10, 883, 1967.

Koiter, W.T., 1963. The effect of axisymmetric imperfections on the buckling of cylindrical shells under axial compression. Proc. Kon. Ned. Ak. Wet. B66, 265.

Lange, C.G., Newell, A.C., 1971. The postbuckling problem for thin elastic shells. SIAM Journal of Applied Mathematics 21, 605–629.

Newell, C., Whitehead, J.A., 1969. Finite band width, finite amplitude convection. Journal of Fluid Mechanics 38, 279–303.

Potier-Ferry, M., 1983. Amplitude modulation, phase modulation and localization of buckling patterns. In Collapse: The buckling of Structure in Theory and Practice, ed. J. M. T. Thompson and G. W. Hunt. Cambridge University Press, Cambridge, pp. 149–159.

Segel, L., 1969. Distant side walls cause slow amplitude modulation of cellular convective. Journal of Fluid Mechanics 38, 203–224.

Thompson, J.M.T., Hunt, G.W., 1973. A General Theory of Elastic Stability. John Wiley, London.

Timoshenko, S.P., Gere, M.C., 1961. Theory of Elastic Stability. McGraw-Hill, New York.

Yamaki, N., 1984. Elastic Stability of Circular Cylindrical Shells. North-Holland, Amsterdam.